We are IntechOpen, the world's leading publisher of Open Access books Built by scientists, for scientists

6,900
Open access books available

185,000
International authors and editors

200M
Downloads

Our authors are among the

154
Countries delivered to

TOP 1%
most cited scientists

12.2%
Contributors from top 500 universities



WEB OF SCIENCE™

Selection of our books indexed in the Book Citation Index in Web of Science™ Core Collection (BKCI)

Interested in publishing with us?
Contact book.department@intechopen.com

Numbers displayed above are based on latest data collected.
For more information visit www.intechopen.com



Chapter 10

Liquid Crystals for Responsible Photonic Crystals

Sunnam Kim and Seiji Kurihara

Additional information is available at the end of the chapter

http://dx.doi.org/10.5772/intechopen.72654

Abstract

The photonic crystals (PCs) exhibit photonic band gap (PBG), inhibiting specific wavelength of light decided by structural periodicity. PCs are a new class of periodic dielectric media that can provide novel ways to manipulate and control light. Researchers have recently devoted extensive efforts to fabricating PCs with controlled symmetry, size, and defects on a large scale and tuning of PBG. Liquid crystalline (LC) materials exhibiting self-organization, phase transition, and molecular orientation behaviors in response to external stimuli are attracting significant attention for the bottom-up nanofabrication and tuning of advanced photonic materials and devices. Here, we will introduce self-organization of PCs from LCs and photoswitching mechanism of PBG based on phase transition and anisotropic orientation of LCs.

Keywords: self-organization, molecular orientation, liquid crystal, azobenzene, light response, photonic band gap

1. Introduction

The structural coloration is basically caused by interaction between light and periodic nanostructured-materials, and light absorption with dyes or pigments is not required for the structural coloration. One can find structural coloration of various materials in nature, and the structural colors are iridescent and very durable, for example, opal, peacock wings, and so on. Recently, there is an increasing interest in developing bioinspired nanostructures with controlled symmetry, size, and defects on a large scale for photonic crystals (PCs) [1–7]. Generally, the fabrication processes are divided into bottom-up and top-down methods. The top-down methods are mostly based on lithography-related techniques, which are expensive and requiring high technology [8–11]. The bottom-up methods are primarily about the self-assembly of component units such as emulsions, colloidal particles, and block copolymers [12–16].

INTECH
open science | open minds

© 2018 The Author(s). Licensee InTech. This chapter is distributed under the terms of the Creative Commons Attribution License (http://creativecommons.org/licenses/by/3.0), which permits unrestricted use, distribution, and reproduction in any medium, provided the original work is properly cited. CC BY

Liquid crystalline (LC) materials are attracting significant interest on the bottom-up nanofabrication of advanced photonic materials and devices with unique configuration and novel tuning mechanism. LCs undoubtedly represent such a marvelous dynamic system based on molecular reorientation behavior affecting macroscopic properties [17–19]. On the other hand, the responsiveness of LCs to various stimuli such as temperature, light, mechanical force, and electric and magnetic fields as well as chemical and electrochemical reactions can attribute to fascinating tunability of photonic band gap (PBG) in the periodic nanostructure, which provides numerous opportunities in all-optical integrated circuits and next-generation communication system. Here, several examples of self-organized LC nanostructures are introduced, and fabrication of three-dimensional (3D) PCs containing azobenzene LC molecules and photoswitching of PBG are discussed.

2. Self-organized PCs and PBG tuning based on LCs

2.1. Self-organized LC nanostructures

We introduce several examples for the fabrication methods of precisely constructing of PCs using self-organized LC nanostructures of cholesteric LC (ChLC), LC blue phase, and holographic polymer-dispersed LC.

2.1.1. Cholesteric LC

Dissolving a chiral compound in a nematic LC causes helix formation, resulting in the selective reflection of circular light corresponding to the helical pitch and helical sense. The pitch, the distance over which the director field rotates by 2π radians, is sensitive to external stimuli such as temperature, light, electric field, and mechanical stress [20–25]. Kurihara et al. have reported on the photochemical change in transparency as well as the selective reflection of a cholesteric LC (ChLC) resulting from the photoisomerization of a chiral azobenzene compound doped in a host nematic LC [26–31]. It is based on the photochemical change in helical twisting power (HTP) of the chiral azobenzene compounds under irradiation of UV and visible light. A combination of a rigid chiral diol core and azobenzene group led to larger photochemical changes in HTP, resulting in a reversible change of selective reflection over whole range of visible region with faster photochemical switching as shown in **Figure 1**. HTPs of the chiral azobenzene compounds increased or decreased by UV light, and the color change of reflection light was seen even with naked eyes.

On the other hand, Muševič et al. developed ChLC microdroplets, in which the arrangement of ChLC molecules was with parallel anchoring of the LC molecules at the surface. The helical structure of the LC originates from the center of the droplet and gives rise to concentric shells of constant refractive index. The introduction of chirality in ChLCs in the spherical shape resulted in the formation of a multilayered spherical Bragg resonator with an alternation periodic refractive index [32]. This dielectric structure is optically equivalent to the well-known Bragg-onion optical microcavity. In addition, Li et al. reported photoresponsive ChLC droplets with large helical twisting power [33].

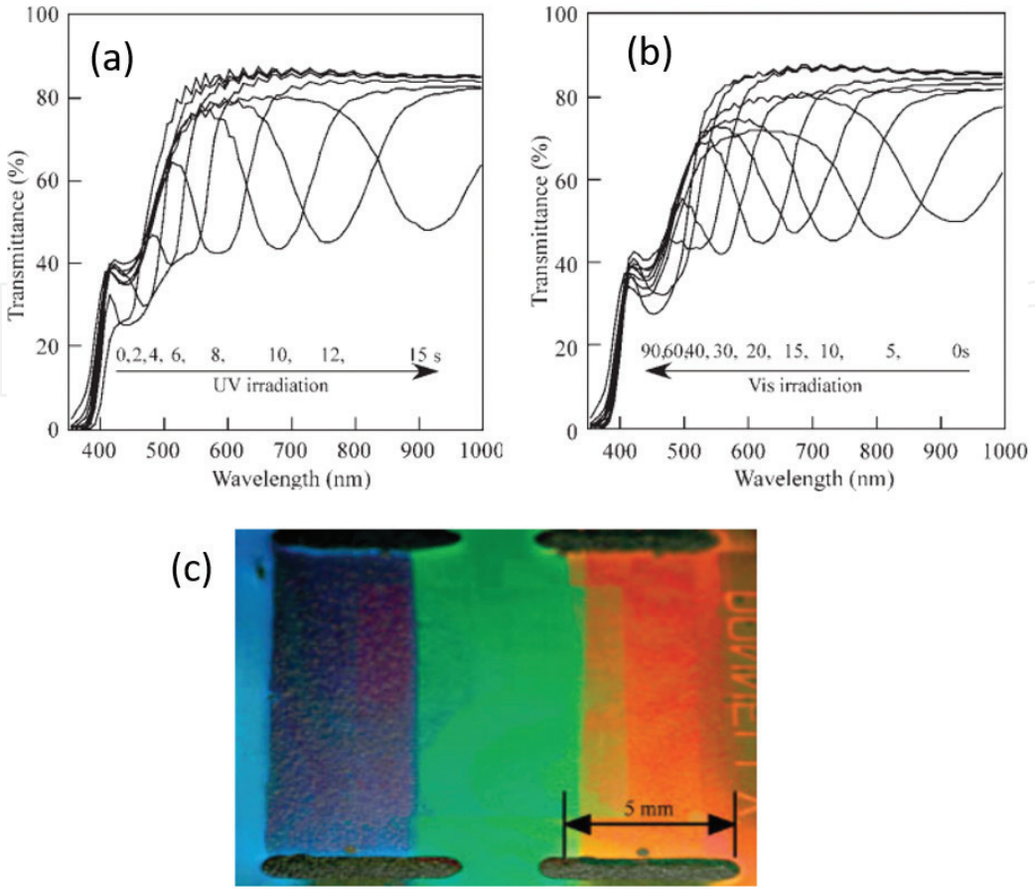


Figure 1. Changes in the selective reflection of the ChLC after UV irradiation (a) and visible light (b) irradiation at 25°C. And the photograph (c) of color change of the ChLC by varying UV irradiation time 0 s (left), 4 s (middle), and 10 s (right). [31] Copyright 2005, Wiley-VCH.

2.1.2. LC blue phase

Blue phases (BPs) are among the most fascinating photonic nanostructures in the area of LCs [34]. They are known to self-organization into the 3D frustrated nanostructures, which originate from the competition between the packing topology and chiral forces. The periodic nanostructures are self-organized from the so-called double-twisted cylinders that are usually stabilized by the formation of defects or disclinations. As the 3D PCs, BPs feature remarkable bandgap tunability over an extensive spectrum in response to various external stimuli such as temperature [35, 36], mechanical strength [37], electric field [38], and light [39–41]. The spectral band gap position of selective reflection can be readily predetermined by varying the chiral fraction of BP mixtures. However, BPs have received increasing attentions especially in recent years, but the reflection wavelength tuning is usually quite narrow. The ability to dynamically tune the photonic bandgap in cubic BPs across a wide wavelength range is highly desirable. Effort to improve the instability and irreversibility of BPs has been made with polymer-stabilized structure [18] and incorporation of unusual bent-core mesogen [42].

2.1.3. Holographic polymer-dispersed LC

Holographic polymer-dispersed liquid crystal (H-PDLC) materials belong to a phase separation material system where the LCs can form droplets, of controllable sizes, that are phase-separated from the polymer-rich regions during the photopolymerization process. Interestingly, it has enabled the in situ fast one-step fabrication of self-organized PCs. The control of the bandwidth of the reflection resonance, related to the light intensity and spatial porosity distributions, was investigated to optimize the optical performance.

For example, Cartwright et al. reported a graded reflection grating based on the H-PDLC material system [43, 44]. An obvious rainbow-colored reflection was observed from the same viewing angle by a modification to this standard configuration where the triangular prism is replaced with a cylindrical lens. Modified optical setup is based on a cylindrical lens to generate a graded holographic interference pattern along the x-axis from the incident and reflected beams. It is expected to compact graded PBG structures for linear variable optical filters.

The marriage of holography and self-organized LC materials is highly expected to produce a diverse range of novel 1D, 2D, and 3D nanostructures for various applications in electro-optical filters, wavelength division multiplexer, free-space optical switches, information display devices, and so on [45–49].

2.2. PBG tuning of 3D photonic crystals

Three-dimensional PCs such as opal and inverse opal structure can be easily prepared by colloidal self-assembly approach. The fabrication of inverse opal structure infiltrated by azobenzene LC molecules for 3D PCs and the mechanism of photoswitching of PBG are described.

For 3D PCs, the reflection wavelength (λ) under normal incident condition is expected by equation of Bragg diffraction as follows [50]

$$\lambda = 2\sqrt{\frac{2}{3}}\, d \sqrt{n_{sphere}{}^2 f + n_{void}{}^2 (1-f)} \tag{1}$$

where d is the diameter of the sphere, n_{sphere} and n_{void} are the refractive indices of the sphere and the medium in the voids of opal, respectively, and f is the volume fraction of the sphere. In this way, the peak wavelength can be roughly tuned by two approaches: either by control of the diameter of the sphere or by control of the refractive index. If one can control photochemically phase transition or birefringence of LCs in 3D PCs, they will be candidates for applications to optical devices such as display and memory.

On the other hand, light among various promising stimuli shows distinct and significant advantages due to its spatial, remote, and temporal controllability. It is also noteworthy that the light sources with different wavelength, intensity, and polarization are readily accessible. Photocontrol of chemical and physical functions of various molecular systems has been studied vigorously using photochemical configurational change of azobenzene derivatives [51–54]. The photochromism of azobenzene and its derivatives due to cis-trans isomerization has been widely investigated. For PC containing azobenzene molecules, 'photochemical

phase transition' between the alignment phase and isotropic phase, or 'photoinduced optical anisotropy' based on photoselective reorientation behavior is very useful parameter for self-organization and optical photonic crystal switching. Here, fabrication of three-dimensional (3D) PC containing azobenzene molecules and photoswitching of PBG are discussed.

2.2.1. PBG tuning by phase transition change

Three-dimensional PCs such as opal and inverse opal structure can be infiltrated with stimuli-responsive materials, thus enabling PBG tuning. Kubo et al. reported on the drastic change in optical properties for the inverse opal structure containing low molar mass LCs, by taking advantage of the nematic-isotropic phase transition [50]. It is based on change in the light scattering intensity between LC phase and isotropic phase.

SiO_2 inverse opal template could be fabricated by infiltration of SiO_2 spheres into the voids of polystyrene (PS) opal film and calcination of PS as shown in **Figure 2**. When SiO_2 inverse opal film infiltrated with 4-cyano-4′-pentylbiphenyl (5CB), the reflection spectra of the LC-infiltrated inverse opal film were changed with increase in the temperature as shown in **Figure 3**. In the initial state at 25°C, 5CB is in the nematic phase and the film is white due to light scattering. The reflection has two weak peaks. With the gradual temperature rise, the positions of the peaks shifted slowly and a distinct peak at around 610 nm, which is derived

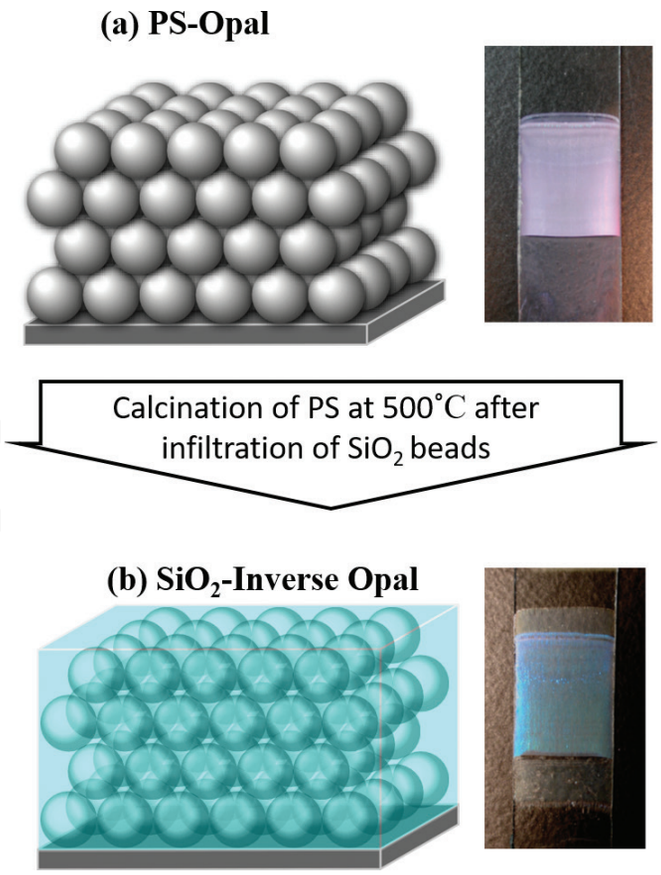


Figure 2. Schematic of PS opal (a) and SiO_2 inverse opal (b) structures and their photographs.

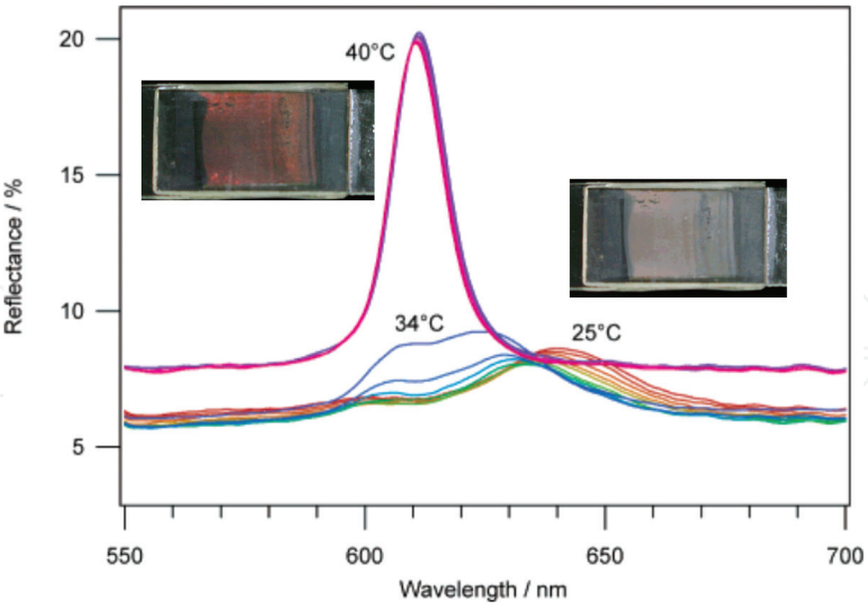


Figure 3. Reflection spectra of SiO_2 inverse opal film infiltrated with 5CB at the temperature from 25°C to 40°C [50]. Reproduced. Copyright 2004, American Chemical Society.

from PBG, appeared rapidly at the phase transition temperature into the isotropic phase at 40°C. The color of film becomes red. This result shows that switching of the optical properties can be realized due to a phase transition of the LCs, leading to thermos-tunable PCs.

Kubo et al. also reported the photoswitching of reflection for SiO_2 inverse opal film infiltrated with photo-response azobenzene containing LC mixture [55]. By UV light, a reflection peak increased rapidly and then saturated, indicating appearance of PBG. The trigger for this drastic change was the trans-cis photoisomerization of the azobenzene derivatives in the films. The excitation of the π-π^* transition of azobenzene molecules at around 360 nm results in a transformation from trans to cis isomers. The photoinduced cis form of azobenzene group has a bent shape and hence tends to disorganize the phase structure of nematic LCs.

The observed change could be reversed to the original state, decrease of reflectance, by irradiating with visible light. The recovery was induced by cis-trans photoisomerization, followed by a phase transition from the isotropic to the nematic phase under visible light (436 nm). Such a switching effect could also be observed in transmission spectra. It is supposed due to the fact that the LC molecules in the nematic phase in the spheroidal voids are aligned parallel to the void surfaces, but the orientation is completely random among spheres. It is similar to the phenomena observed for polymer-dispersed liquid crystal (PDLC). On the other hand, when the LC was transformed into an isotropic phase by UV light, the anisotropy in the dielectric constant disappeared. That is, the dielectric constant of the LC in all of the spheroidal voids became the same, and hence, a reflection peak due to Bragg diffraction appears [56–58]. On the basis of this scenario, dynamic change in the optical properties was observed repeatedly by alternating irradiation with UV and visible light. It was completely reversible, exhibiting good stability and reproducibility during the light irradiation cycle as shown in **Figure 4**.

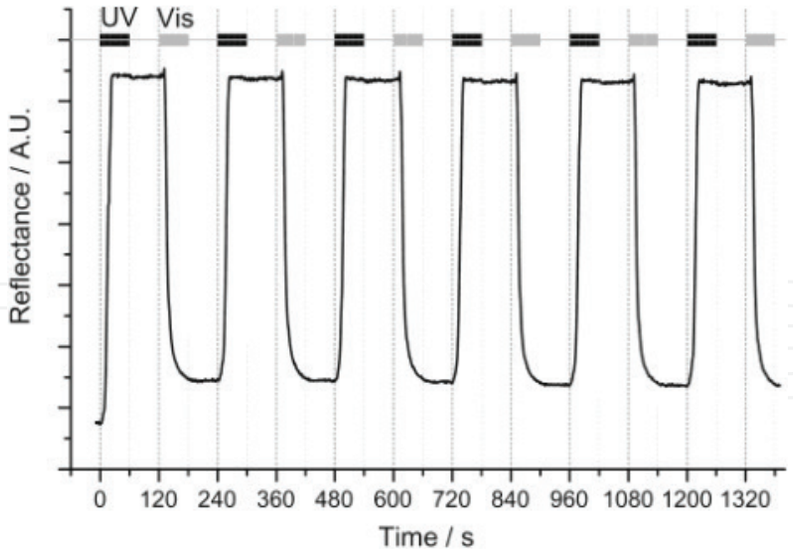


Figure 4. Time-dependent change in the reflectance of 5CB/azobenzene LC mixture-infiltrated inverse opal film at 603 nm by UV and visible light irradiation. The black bars show the periods for the irradiation of UV light (<400 nm), and the gray bars show the periods for irradiation of visible light (436 nm). For other periods, the sample was kept in the dark [58]. Copyright 2002, American Chemical Society.

2.2.2. PBG tuning by molecular reorientation

For low-molar-mass LC-infiltrated inverse opal film as mentioned in the previous section, the stability of the switched state was not enough although the photoswitching was reversible. It is due to the thermal back reaction of the azobenzene compound and fluidity of the low-molar-mass LC. In contrast with low-molar-mass LCs, polymeric LCs are well known to show excellent storage stability. Kurihara et al. reported the stable and reversible shift of the Bragg diffraction band for SiO_2 inverse opal structure infiltrated with 4,4′-methoxy hexyloxy azobenzene polymethacrylate, PAz (schematic molecular structure is shown in **Figure 5**), and reflection change were investigated when irradiation of linearly polarized light (LPL) and circularly polarize light (CPL) of Ar + later (λ = 488 nm) [59].

Photoisomerization behavior is demonstrated by absorption band change as shown in **Figure 6**. By UV light, trans-cis isomerization is induced, the absorption peak at 360 nm decreases, and the peak at 450 nm increases (**Figure 5(a)** and **(c)**). By irradiation of visible light, cis-trans photoisomerization is induced, and reverse changes in absorption spectra are induced (**Figure 6(b)** and **(d)**).

Anisotropic state of azobenzene compounds based on their molecular orientation can be controlled via reversible isomerization behavior by light and thermal stimuli [60–62]. Namely, alignment state of trans-form is perpendicular to the direction of polarized light (known as Weigert effect [20, 63–64]), and the alignment is destroyed by formation of cis-form.

The orientation state is evaluated by polarized absorption spectra and by birefringence, Δn, measurement. From angle dependence of absorbance at the peak of 360 nm to the polarized axis, orientation direction perpendicular to the polarized direction of induced LPL was demonstrated. When Δn is estimated by change in transmitted light of the azobenzene film

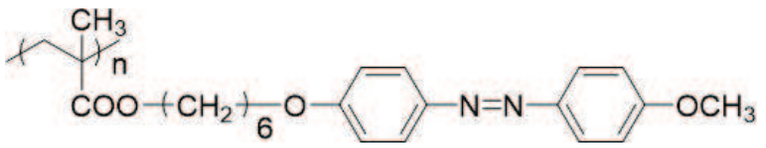


Figure 5. Schematic molecular structure of PAz.

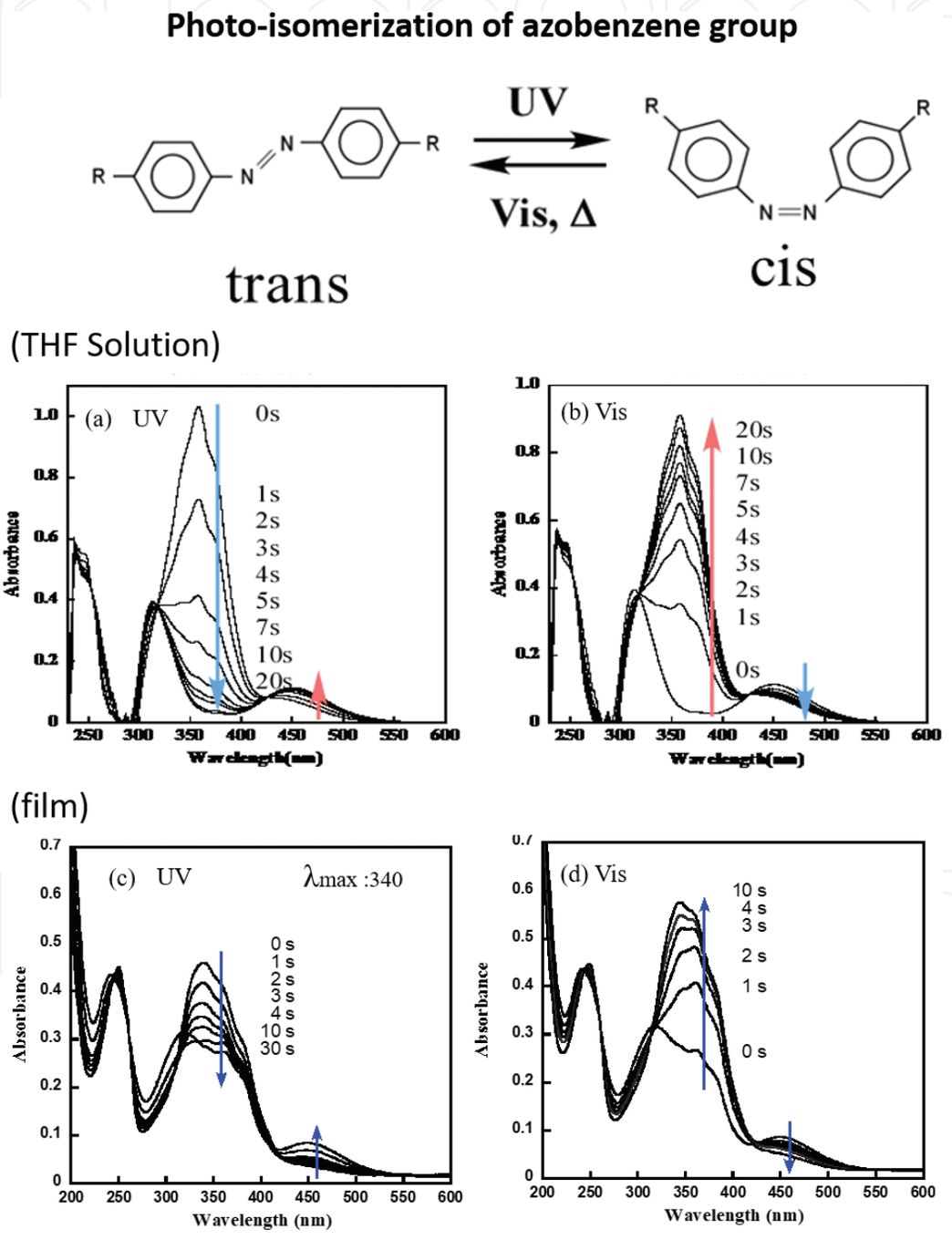


Figure 6. Changes in absorption spectra of PAz in THF after UV light (365 nm, 8 mW/cm^2) (a) and visible light (436 nm, 60 mW/cm^2) (b) irradiation. Changes in absorption spectra of PAz film irradiated UV light (365 nm, 10 mW/cm^2) (c) and following visible light (436 nm, 58 mW/cm^2) (d) at room temperature.

placed between two crossed polarizers, Δn of PAz was estimated to be 0.128, as shown in **Figure 7** [65].

Azobenzene polymer can be infiltrated into the SiO_2 inverse opal film by heating to melt. The pore diameter and volume fraction of SiO_2 inverse opal, d and f, were estimated by comparing wavelength of the reflection peaks of the SiO_2 inverse opal films infiltrated with various solvents with different refractive indices. For SiO_2 inverse opal film, d = 278 nm and f = 0.118, reflection spectra before and after injection of PAz are shown in **Figure 8**. The injection of PAz caused a shift of the reflection peak from 480 nm to 710 nm, because of an increase in the refractive index from 1.0 of air to 1.6 of PAz.

By LPL irradiation of light, reflection measured with polarizer parallel and perpendicular to the polarization direction of LPL is plotted in **Figure 9**. The reflection peaks depend on the irradiation time and polarization direction. By irradiation of a linearly polarized light at 488 nm (Ar + laser), azobenzene groups were aligned in the direction perpendicular to the polarization direction of the laser light.

After irradiation of LPL, reflection band shifted to longer wavelength with little shoulder at shorter wavelength. By observation with parallel and perpendicular polarizers, different two bands were respectively observed. The maximum wavelengths of the reflection bands at shorter and longer wavelength regions were 706 nm and 725 nm, respectively. Therefore, the refractive indices of PAz in the pores after the LPL irradiation, ordinary refractive index (n_o) and extraordinary refractive index (n_e), were estimated to be, respectively, 1.57 and 1.62 by using Bragg diffraction (Eq. (1)) with the parameters d (278 nm), f (0.118), and $nSiO_2$ (1.45). Namely, the photoinduced birefringence of PAz was 0.05 in the pores of SiO_2 inverse opal. It is less optical anisotropy comparing to solid film of PAz (0.13), indicating insufficient alignment

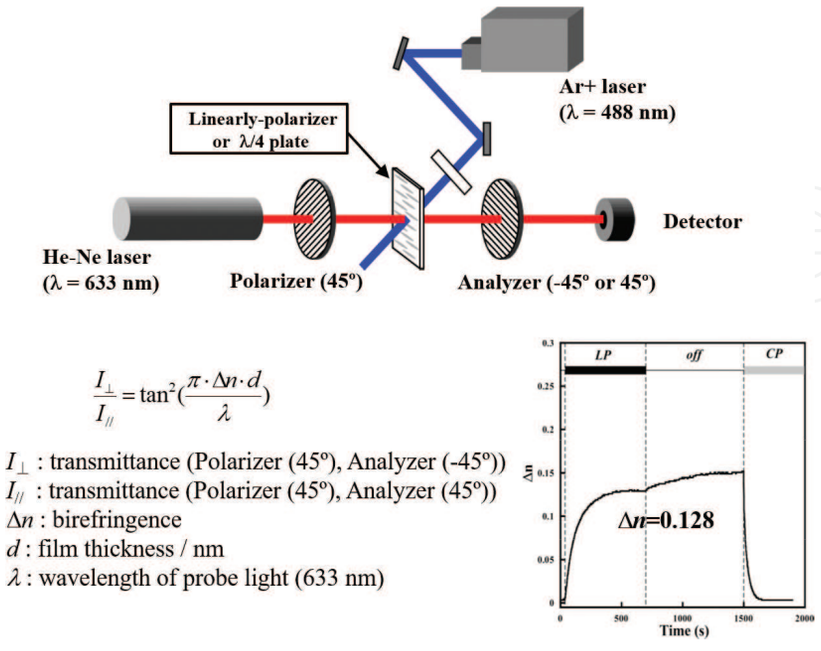


Figure 7. Schematic for birefringence measurement and the result of PAz.

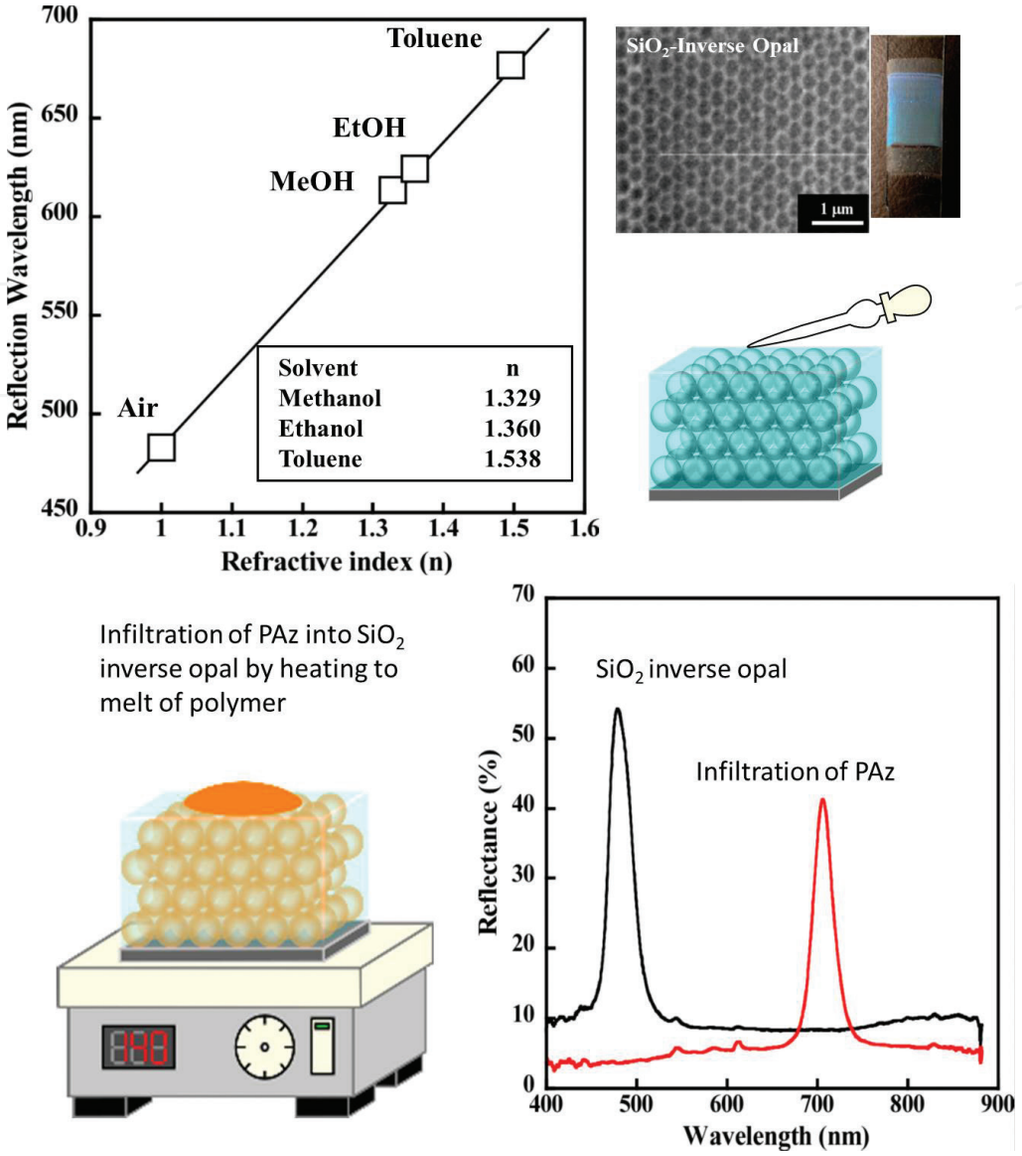


Figure 8. Plot of reflection wavelength change of SiO_2 inverse opal structure depending on solvents with various refractive indices (a) and reflection spectra before and after infiltration of PAz (b).

due to huge surface energy in the pores of SiO_2. In addition, reflection intensity decreased and increased by small and larger refractive index differences between PAz (1.57 and 1.62) and SiO_2 (1.45).

3. Conclusion

Optical properties of LCs represent the responsibility of external stimuli such as temperature, light, mechanical force, and electric and magnetic fields as well as chemical and electrochemical reactions, which are a driving force leading to dynamic change of materials from molecular level to macroscopic level. Dynamic system of LCs makes it a quite advantageous

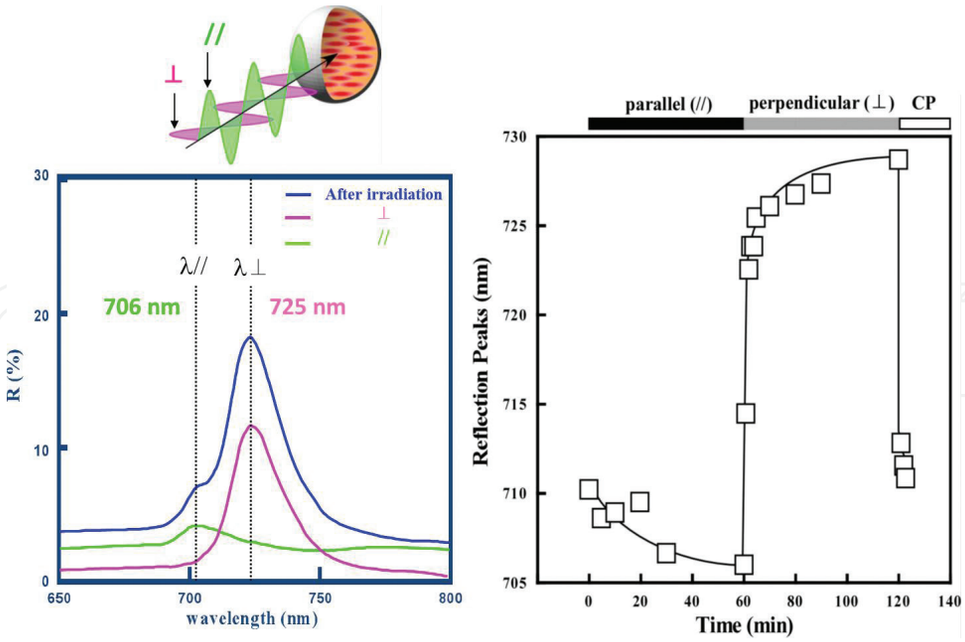


Figure 9. Reflection spectra of Paz-infiltrated SiO_2 film with parallel and perpendicular LPL irradiation of Ar + laser and plot of the wavelength of reflection peak [59].

approach toward bottom-up nanofabrication of photonic materials with novel tuning mechanism. In addition, the responsiveness to various stimuli can attribute to fascinating tunability of PBG, which provides numerous opportunities in all-optical integrated circuits and next-generation communication system.

Author details

Sunnam Kim* and Seiji Kurihara

*Address all correspondence to: sn-kim@kumamoto-u.ac.jp

Department of Applied Chemistry and Biochemistry, Kumamoto University, Kumamoto, Japan

References

[1] Zan G, Wu Q. Biomimetic and bioinspired synthesis of nanomaterials/nanostructures. Advanced Materials (Deerfield Beach, Fla.). 2016;**28**:2099-2147

[2] Pokroy B, Epstein AK, Persson-Gulda MCM, Aizenberg J. Fabrication of bioinspired actuated nanostructures with arbitrary geometry and stiffness. Advanced Materials. 2009;**21**:463-469

[3] Pris AD, Utturkar Y, Surman C, Morris WG, Vert A, Zalyubovskiy S, et al. Towards high-speed imaging of infrared photons with bio-inspired nanoarchitectures. Nature Photonics. 2012;**6**:195-200. DOI: 10.1038/nphoton.2011.355

[4] Bai L, Xie Z, Wang W, Yuan C, Zhao Y, Mu Z, et al. Bio-inspired vapor-responsive colloidal photonic crystal patterns by inkjet printing. ACS Nano. 2014;**8**:11094-11100

[5] Ye B, Rong F, Gu H, Xie Z, Cheng Y, Zhao Y, et al. Bioinspired angle-independent photonic crystal colorimetric sensing. Chemical Communications. 2013;**49**:5331-5333

[6] Hou J, Zhang H, Yang Q, Li M, Song Y, Jiang L. Bio-inspired photonic-crystal microchip for fluorescent ultratrace detection. Angewandte Chemie International Edition. 2014;**53**:5791-5795

[7] Biró LP, Vigneron JP. Photonic nanoarchitectures in butterflies and beetles: Valuable sources for bioinspiration. Laser & Photonics Reviews. 2011;**5**:27-51

[8] Campbell M, Sharp DN, Harrison MT, Denning RG, Turberfield AJ. Fabrication of photonic crystals for the visible spectrum by holographic lithography. Nature. 2000;**404**:53-56

[9] Blanco A, Chomski E, Grabtchak S, Ibisate M, John S, Leonard SW, et al. Large-scale synthesis of a silicon photonic crystal with a complete three-dimensional bandgap near 1.5 micrometres. Nature. 2000;**405**:437-440

[10] Deubel M, Freymann G von, Wegener M, Pereira S, Busch K, Soukoulis CM. Direct laser writing of three-dimensional photonic-crystal templates for telecommunications. Nature Materials 2004;**3**:444-447

[11] Qi M, Lidorikis E, Rakich PT, Johnson SG, Joannopoulos JD, Ippen EP, et al. A three-dimensional optical photonic crystal with designed point defects. Nature. 2004;**429**:538-542

[12] Hynninen A-P, Thijssen JHJ, Vermolen ECM, Dijkstra M, van Blaaderen A Self-assembly route for photonic crystals with a bandgap in the visible region. Nature Materials 2007; **6**:202-205

[13] Jenekhe S, Chen X. Self-assembly of ordered microporous materials from rod-coil block copolymers. Science. 1999;**283**:372-375

[14] Vlasov YA, Bo X-Z, Sturm JC, Norris DJ. On-chip natural assembly of silicon photonic bandgap crystals. Nature. 2001;**414**:289-293

[15] Winfree E, Liu F, Wenzler LA, Seeman NC. Design and self-assembly of two-dimensional DNA crystals. Nature. 1998;**394**:539-544

[16] Joannopoulos JD. Photonics: Self-assembly lights up. Nature. 2001;**414**:257-258

[17] Gibbons WM, Shannon PJ, Sun S-T, Swetlin BJ. Surface-mediated alignment of nematic liquid crystals with polarized laser light. Nature. 1991;**351**:49-50

[18] Kikuchi H, Yokota M, Hisakado Y, Yang H, Kajiyama T. Polymer-stabilized liquid crystal blue phases. Nature Materials. 2002;**1**:64-68

[19] Shannon PJ, Gibbons WM, Sun ST. Patterned optical properties in photopolymerized surface-aligned liquid-crystal films. Nature. 1994;**368**:532-533

[20] Ikeda T, Sasaki T, Ichimura K. Photochemical switching of polarization in ferroelectric liquid-crystal films. Nature. 1993;**361**:428-430

[21] Kurihara S, Nomiyama S, Nonaka T. Photochemical control of the macrostructure of cholesteric liquid crystals by means of photoisomerization of chiral azobenzene molecules. Chemistry of Materials. 2001;**13**:1992-1997

[22] Huang Y, Zhou Y, Doyle C, Wu S-T. Tuning the photonic band gap in cholesteric liquid crystals by temperature-dependent dopant solubility. Optics Express. 2006;**14**:1236-1242

[23] Moreira M et al. Cholesteric liquid-crystal laser as an optic fiber-based temperature sensor. Applied Physics Letters. 2004;**85**:2691-2693

[24] Baessler H, Laronge TM, Labes MM. Electric field effects on the optical rotatory power of a compensated cholesteric liquid crystal. The Journal of Chemical Physics. 1969;**51**:3213-3219

[25] Finkelmann H, Kim ST, Munoz A, Palffy-Muhoray P, Taheri B. Tunable mirrorless lasing in cholesteric liquid crystalline elastomers. Advanced Materials. 2001;**13**:1069-1072

[26] Kurihara S et al. Photo-tuning of lasing from a dye-doped cholesteric liquid crystals by photoisomerization of a sugar derivative having plural azobenzene groups. Applied Physics Letters. 2006;**88**:103121

[27] Hatae Y, Moritsugu M, Ogata T, Kurihara S, Nonaka T. Photochemical modulation of the wavelength of lasing from a dye-doped cholesteric liquid crystal. Molecular Crystals and Liquid Crystals. 2005;**443**:87-94

[28] Yoshioka T, Alam MZ, Ogata T, Nonaka T, Kurihara S. Photochemical tuning of the helical structure of cholesteric liquid crystals by photoisomerization of chiral azobenzenes, and their structural effects. Liquid Crystals. 2004;**31**:1285-1291

[29] Yoshioka T, Ogata T, Zahangir AM, Nonaka T. Discontinuous change in the helical pitch of cholesteric liquid crystals by photoisomerization of a chiral azobenzene molecule. Liquid Crystals. 2004;**31**:15-19

[30] Kurihara S, Yoshioka T, Zahangir A, Ogata T, Nonaka T. Preparation of composites of polymer liquid crystal/cholesteric liquid crystal and their photochemical switching and memory properties by photoisomerization of a chiral azobenzene molecule. Journal of Applied Polymer Science. 2004;**92**:2577-2580

[31] Yoshioka T et al. Reversible-photon-mode full-color display by means of photochemical modulation of a helically cholesteric structure. Advanced Materials. 2005;**17**:1226-1229

[32] Humar M, Muševič I. 3D microlasers from self-assembled cholesteric liquid-crystal microdroplets. Optics Express. 2010;**18**:26995-27003

[33] Chen L et al. Photoresponsive monodisperse cholesteric liquid crystalline microshells for tunable omnidirectional lasing enabled by a visible light-driven chiral molecular switch. Advanced Optical Materials. 2014;**2**:845-848

[34] Cao W, Muñoz A, Palffy-Muhoray P, Taheri B. Lasing in a three-dimensional photonic crystal of the liquid crystal blue phase II. Nature Materials. 2002;**1**:111-113

[35] Hur S-T et al. Liquid-crystalline blue phase laser with widely tunable wavelength. Advanced Materials. 2013;**25**:3002-3006

[36] Coles H, Pivnenko M. Liquid crystal 'blue phases' with a wide temperature range. Nature. 2005;**436**:997-1000

[37] Castles F et al. Stretchable liquid crystal blue phase gels. Nature Materials. 2014;**13**:817-821

[38] Lu S, Chien L. Electrically switched color with polymer-stabilized blue-phase liquid crystals. Optics Letters. 2010;**35**:562-564

[39] Lin T-H et al. Red, green and blue reflections enabled in an optically tunable self-organized 3D cubic nanostructured thin film. Advanced Materials. 2013;**25**:5050-5054

[40] Wang L et al. NIR light-directing self-organized 3D photonic superstructures loaded with anisotropic plasmonic hybrid nanorods. Chemical Communications. 2015;**51**:15039-15042

[41] Chen X et al. Light-controllable reflection wavelength of blue phase liquid crystals doped with azobenzene-dimers. Chemical Communications. 2013;**49**:10097-10099

[42] Lee M et al. Liquid crystalline blue phase I observed for a bent-core molecule and its electro-optical performance. Journal of Materials Chemistry. 2010;**20**:5813-5816

[43] Liu K, Xu H, Hu H, Gan Q, Cartwright AN. One-step fabrication of graded rainbow-colored holographic photopolymer reflection gratings. Advanced Materials. 2012;**24**:1604-1609

[44] Moein T et al. Holographic photopolymer linear variable filter with enhanced blue reflection. ACS Applied Materials & Interfaces. 2014;**6**:3081-3087

[45] Coles H, Morris S. Liquid-crystal lasers. Nature Photonics. 2010;**4**:676-685

[46] Jakubiak R, Bunning TJ, Vaia RA, Natarajan LV, Tondiglia VP. Electrically switchable, one-dimensional polymeric resonators from holographic photopolymerization: A new approach for active photonic bandgap materials. Advanced Materials. 2003; **15**:241-244

[47] Escuti MJ, Qi J, Crawford GP. Tunable face-centered-cubic photonic crystal formed in holographic polymer dispersed liquid crystals. Optics Letters. 2003;**28**:522-524

[48] He GS et al. Tunable two-photon pumped lasing using a holographic polymer-dispersed liquid-crystal grating as a distributed feedback element. Applied Physics Letters. 2003;**83**:2733-2735

[49] Wu S, Fuh A. Lasing in photonic crystals based on dye-doped holographic polymer-dispersed liquid crystal reflection gratings. Japanese Journal of Applied Physics. 2005;**44**:977

[50] Kubo S et al. Tunable photonic band gap crystals based on a liquid crystal-infiltrated inverse opal structure. Journal of the American Chemical Society. 2004;**126**:8314-8319

[51] Shinkai S, Nakaji T, Nishida Y, Ogawa T, Manabe O. Photoresponsive crown ethers. 1. Cis-trans isomerism of azobenzene as a tool to enforce conformational changes of crown ethers and polymers. Journal of the American Chemical Society. 1980;**102**:5860-5865

[52] Ogawa M. Preparation of a cationic azobenzene derivative-montmorillonite intercalation compound and the photochemical behavior. Chemistry of Materials. 1996;**8**:1347-1349

[53] Seki T et al. Photochemical alignment regulation of a nematic liquid crystal by Langmuir-Blodgett layers of azobenzene polymers as "command surfaces". Macromolecules. 1989;**22**:3505-3506

[54] Ikeda T, Tsutsumi O. Optical switching and image storage by means of azobenzene liquid-crystal films. Science. 1995;**268**:1873-1875

[55] Kubo S et al. Control of the optical properties of liquid crystal-infiltrated inverse opal structures using photo irradiation and/or an electric field. Chemistry of Materials. 2005;**17**:2298-2309

[56] Tarhan İİ, Watson GH. Photonic band structure of fcc colloidal crystals. Physical Review Letters. 1996;**76**:315-318

[57] Park SH, Xia Y. Assembly of mesoscale particles over large areas and its application in fabricating tunable optical filters. Langmuir. 1999;**15**:266-273

[58] Kubo S, Gu Z, Takahashi K, Ohko Y, Sato O, Fujishima A. Control of the optical band structure of liquid crystal infiltrated inverse opal by a photoinduced nematic–isotropic phase transition. Journal of the American Chemical Society. 2002;**124**:10950-10951

[59] Kurihara S et al. Photoswitching properties of photonic band gap material containing azo-polymer liquid crystal. European Polymer Journal. 2007;**43**:4951-4960

[60] Natansohn A, Rochon P. Photoinduced motions in azo-containing polymers. Chemical Reviews. 2002;**102**:4139-4176

[61] Alam Z, Ohmachi T, Ogata T, Nonaka T. Kurihara S, Photoisomerization behavior and photoinduced surface relief gratings on azopolymer film by a monochromatic light irradiation. Optical Materials. 2006;**29**:365-370

[62] Kim S, Ogata T, Kurihara S. Azobenzene-containing polymers for photonic crystal materials. Polymer Journal. 2017;**49**:407-412

[63] Shishido A. Rewritable holograms based on azobenzene-containing liquid-crystalline polymers. Polymer Journal. 2010;**42**:525-533

[64] Ichimura K, Suzuki Y, Seki T, Hosoki A, Aoki K. Reversible change in alignment mode of nematic liquid crystals regulated photochemically by command surfaces modified with an azobenzene monolayer. Langmuir. 1988;**4**:1214-1216

[65] Ishiguro M, Sato D, Shishido A, Ikeda T. Bragg-type polarization gratings formed in thick polymer films containing azobenzene and tolane moieties. Langmuir. 2007;**23**:332-338

IntechOpen

IntechOpen